

## Tsunami fragility curves for seaport structures

S. V. Karafagka<sup>1</sup>, S.D. Fotopoulou, K.D. Pitilakis  
*Aristotle University, Thessaloniki, Greece*

### ABSTRACT

The recent devastating tsunami events and the future higher impact expected due to the increasing number of people and structures being exposed to tsunami hazards revealed the need for the estimation of the effects of tsunamis especially on seaport structures. This study aims at developing analytical tsunami fragility functions for some representative typologies of seaport structures in Greece. An extensive numerical parametric investigation has been performed considering different combinations of tsunami loads based on FEMA (2008) recommendations for gradually increasing tsunami inundation depths and for the various structure typologies. Tsunami nonlinear static analyses have been performed and appropriate tsunami capacity curves have been derived. Structural limit states have been defined on tsunami capacity curves in terms of threshold values of material strain. Fragility curves have been numerically calculated for different damage states with gradually increasing inundation depths using nonlinear regression analysis. They could be used within a probabilistic risk assessment framework to assess the vulnerability of typical seaport structures exposed to tsunami hazard along European-Mediterranean and other regions of similar facilities worldwide.

*Keywords: Tsunami fragility curves, Tsunami capacity curves, Damage states, Port structures*

### INTRODUCTION

Tsunamis are long-period water waves that can be triggered by undersea earthquakes, landslides or volcanic eruptions. Occurrence of tsunamis can cause tremendous direct and indirect losses in terms of human lives building and infrastructure damage as seen recently in Japan after the 2011 Great East earthquake, Chile 2010 and in the coastlines of the Indian Ocean 2004 (e.g. Suppasri et al., 2013; Mas et al., 2012; Koshimura et al., 2009). However, only a limited number of tools to estimate the potential impacts of tsunami to structures are available until now. Existing tsunami fragility functions for buildings and infrastructures are principally based on empirical data from previous tsunami events and/or expert judgment (Reese et al., 2011; Suppasri et al., 2011; 2013; etc.).

To bridge the gap, this study aims at developing analytical tsunami fragility functions for the vulnerability assessment of some representative typologies of seaport structures. In particular, low-code MRF and dual RC buildings of various heights (considering or not infills) and a typical warehouse have been considered in the analysis, all representative of the seaport facilities of one of the largest ports in the Aegean Sea basin, the port of Thessaloniki in Greece. To minimize the uncertainties related to the definition of damage limit states, tsunami nonlinear static analyses have been performed for gradually increasing tsunami inundation depths and appropriate tsunami capacity curves have been derived. Structural limit states have been defined on tsunami capacity curves in terms of threshold values of material strain. The outcome of the parametric study is the derivation of fragility curves, which describe the probability of exceeding a certain limit state of the structure, with the inundation depth. Lognormally distributed fragility curves are finally derived as a function of the

---

<sup>1</sup> Corresponding Author: S.V. Karafagka, Aristotle University, Thessaloniki, Greece, [stellak@civil.auth.gr](mailto:stellak@civil.auth.gr)

inundation depth. A preliminary comparison was carried out with available empirical fragility curves obtained using field survey data from the 2011 Great East Japan tsunami, which however concern relatively different typologies of structures.

## METHODOLOGY

The proposed methodology, largely inspired from earthquake risk analysis, is applicable for the vulnerability assessment of buildings subjected to tsunami forces. It is based on a comprehensive set of numerical computations and adequate statistical analysis. The framework of the proposed methodology is schematically illustrated in Fig.1.

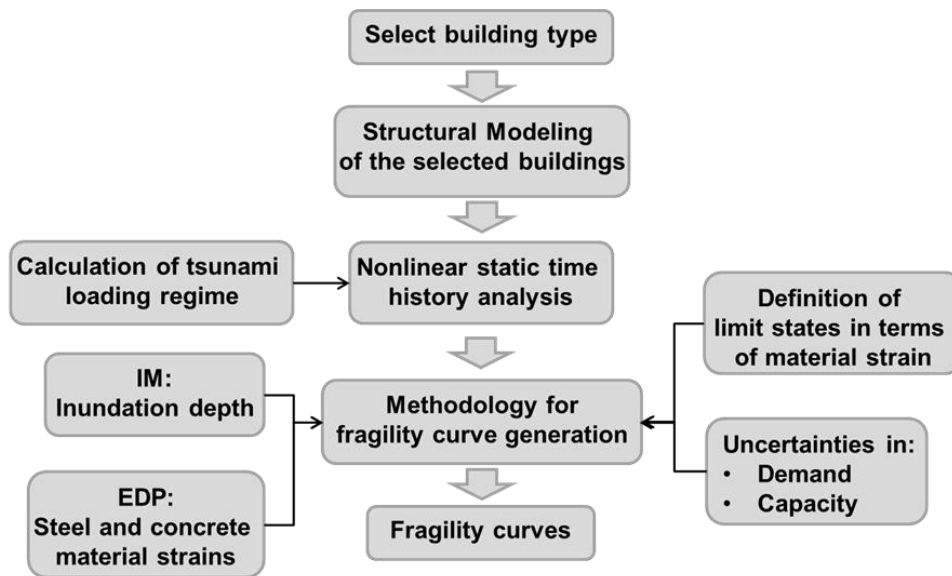


**Figure 1.** Flowchart of the proposed methodology

Several building typologies (i.e. low-code RC buildings and a typical warehouse) representative of Thessaloniki's port critical structures were considered to apply the proposed method. Nonlinear constitutive models were used to simulate the behaviour of materials since cracking and irreversible deformations are normally expected to govern the building's response. It should be noted that all models are fixed-base. It is also worth noting that in this phase of the study (single-risk assessment), far-source generated tsunami is considered, where the epicentre of the earthquake is assumed to be at a long distance from the structure and the structure has not sustained any initial damage due to ground shaking.

Tsunami loading was determined based on FEMA (2008) recommendations and proper engineering judgment. In particular, each structure was subjected to buoyant, hydrostatic and hydrodynamic forces combined with forces due to debris, all of which constitute tsunami load effects. The considered combination of tsunami forces differs for the various building typologies whereas the amplitude of the resultant force increases with increasing tsunami inundation depth. Tsunami flows consist of a mixture of sediment and seawater. Based on an assumption of vertically averaged sediment-volume concentration of 10% in seawater, the fluid density of tsunami flow is taken as 1.2 times the density of fresh water ( $1.200 \text{ kg/m}^3$ ). Also, it is assumed that tsunami flow cannot enter the building for the case of models with masonry infills (watertight walls) and tsunami cannot completely destroy masonry infills. Watertight floor is considered in all models. Once the leading edge of the surge has passed a structural component, it will no longer experience the impulsive force,  $F_s$ , but rather a sustained hydrodynamic drag force,  $F_d$  (FEMA, 2008). The computations have been carried out with the worst case scenario considering the simultaneous action of all loads and that in particular that the leading edge of the surge fully impacts the most closed off section of the building and the debris impact forces are acting on the structure.

The computed forces are then directly applied as input time-variant static loads to an appropriate nonlinear structural model for gradually increasing inundation depths and the structure's response in terms of material strain (i.e. the engineering demand parameter, EDP) for the different statically applied tsunami loads is

estimated. It is noted that a local damage index, such as material strain, is better correlated with structural damage compared to a global damage index, as e.g. Macabuag et al. (2014). Subsequently, appropriate limit damage states are defined in terms of threshold values of the material strain of the structure, based on nonlinear static analyses for the various typical structures of the port, engineering judgment and the literature (e.g. (Crowley et al., 2004; Fotopoulou & Ptilakis, 2013; Ptilakis, 2015)). Four damage states are proposed in this study associated with none to slight, moderate, extensive and complete structural damage of the structure.

The vulnerability is assessed through probabilistic fragility curves, which describe the probability of exceeding each limit state, considering various sources of uncertainty with respect to the structural capacity and the demand (in terms of material strain). A key point in the derivation of fragility curves is the selection of the intensity measure (IM) that adequately correlates with damage. According to FEMA (2008), it is noted that numerical predictions of flow velocities are less accurate than predictions of inundation depths, and the grid size for numerical simulations in the run-up zone must be very fine in order to obtain sufficient accuracy in velocity predictions. In addition, most existing empirical fragility functions are derived in terms of inundation depth, also recommended by Koshimura et al., (2009), as it is the parameter most easily measured in the field. Based on the above, inundation depth is selected as an IM. For the development of fragility curves, an appropriate relationship between the numerically calculated material strain (i.e. the EDP) and the gradually increasing inundation depths (i.e. the IM) is established through nonlinear regression analysis. Lognormally distributed fragility curves are finally derived as a function of inundation depth for the different damage limit states for the various structure typologies considered.

## **THESSALONIKI PORT INFRASTRUCTURES**

The interruption of functionality of port structures can have severe direct and indirect effects on the economy and on the social and environmental growth of the broader area of interest, in our case the city of Thessaloniki, or even broader, the country of Greece. The Port of Thessaloniki is one of the largest ports in the Aegean Sea basin and functions as a major gateway for the Balkan hinterland and South-Eastern Europe. Its strategic geographical position increases its importance for the trade and the economy of the region, as it is a crucial point for supply chains, import-export trade and transportation.

Critical buildings of Thessaloniki's port mainly consist of low- and pre- code RC buildings and warehouses. The SYNER-G ([www.syner-g.eu](http://www.syner-g.eu)) taxonomy is used to describe the different RC building typologies. In particular, the studied RC buildings were classified according to their structural system (i.e. MRF, dual), their height (i.e. low-rise, mid-rise and high-rise), the existence or not of infill walls (i.e. bare frames, infilled) as well as the seismic design level (i.e. the 1959 Greek seismic code corresponding to low level of seismic design). The warehouses, which are basically industrial steel structures with or without masonry infills, constitute a category of their own. Fig.2 presents representative cross-sections respectively of the studied RC building typologies (Kappos et al., 2006) with/without infills (eight structures in total) and the typical warehouse (without infills) provided by the Thessaloniki Port authorities and reproduced by AUTH.

## **NUMERICAL MODELLING**

Two-dimensional (2D) numerical simulations of the structures are conducted using the fibre-based finite element code Seismostruct v7.0 (SeismoSoft, 2015), which is widely and successfully used in structural earthquake engineering. The RC structures were realistically reproduced in Seismostruct using non-linear constitutive models. Inelastic force-based formulations are implemented for the nonlinear beam-column frame element modeling. Distributed material inelasticity is applied based on the fibre approach to represent the cross-sectional behaviour (Neuenhofer & Filippou, 1997). Each fibre is associated with a uniaxial stress-strain relationship and the sectional stress-strain state of the beam-column elements is obtained through the integration of the nonlinear uniaxial stress-strain response of the individual fibres into which the section is subdivided. In the present analysis, the frame sections have been discretised into 300 fibres. The concrete fibres are modelled based on the uniaxial nonlinear model proposed by Mander (1988), assuming a constant confining pressure for the confined concrete core fibres throughout the entire stress-strain range. For the reinforcement, a uniaxial bilinear stress-strain model with kinematic strain hardening is utilised.

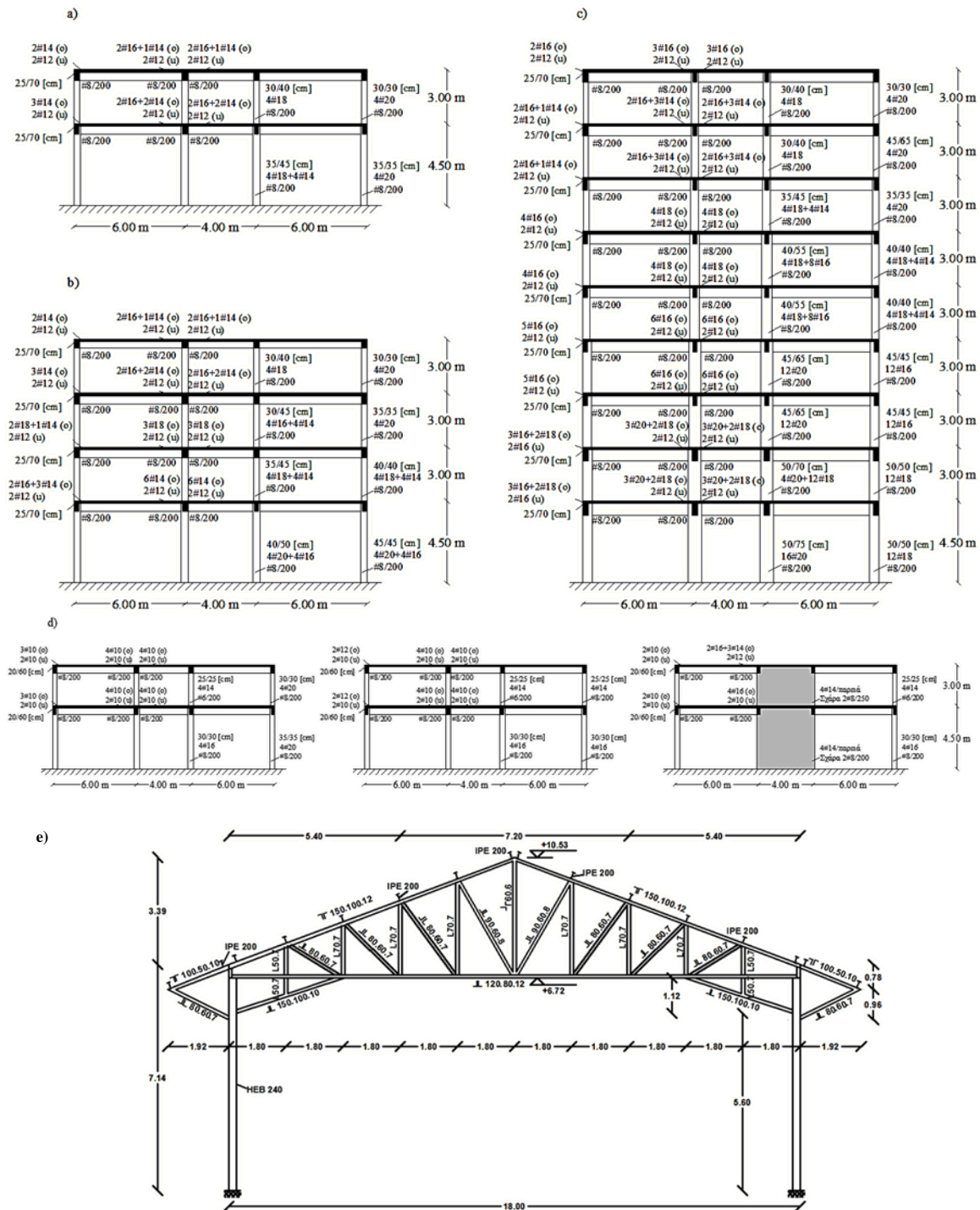


**Figure 2.** Cross-sections of the (a) 2-storey, (b) 4-storey, (c) 9-storey MRF RC buildings and the (d) 2-storey Dual RC building, designed by the 1959 Greek seismic code and the (e) warehouse

The nonlinear response of the masonry panel element in the case of the infilled frame models is simulated based on the double strut model proposed by Crisafulli (1997). Each panel is represented by strut members that carry the axial loads across two opposite diagonal corners and the shear from the top to the bottom of the panel. This latter strut acts only across the diagonal in compression; hence its activation depends on the deformation of the panel. The axial load struts use the masonry strut hysteresis model, while the shear strut uses a dedicated bilinear hysteresis rule, developed by Crisafulli (1997). For the simulation of dual frames, appropriate constraints (i.e. rigid links) are considered to account for the stiffness of the walls. In addition, in models with more than one frame, Equal DOF constraints are used to take into consideration the equal degrees-of-freedom between the frames. Regarding the warehouse modelling, the uniaxial bilinear model with kinematic strain-hardening is employed for the steel material ( $E_s=2.1 \cdot 10^8$  kPa;  $f_y=235000$  kPa;  $\mu=0.01$ ). Columns are modelled using force-based inelastic frame elements (infrmFB) with 4 integration sections, while

trusses are modelled through truss elements (truss). The number of fibres used in section equilibrium computations in both cases is set to 300. The masses are applied as distributed along columns and beams (by assigning the specific weight of steel material) plus concentrated vertical loads on joints due to the existence of trusses on the normal direction.

Tsunami nonlinear static time-history analyses are performed for all numerical simulations. It is noted that an initial static analysis is carried out before the onset of tsunami nonlinear analysis to account for the gravity forces. Tsunami forces calculated according to FEMA (2008) are statically imposed on the structures at the location of each load's resultant depending on the inundation depth ( $d$ ). In particular, the hydrodynamic ( $F_d$ ) and impulsive ( $F_s$ ) forces are applied at  $d/2$  from the base of the structure; the debris impact force ( $F_i$ ) is applied at  $d$  from the base of the structure while the hydrostatic forces ( $F_h$ ) are applied at  $d/3$  from the base of the structure. Buoyant forces ( $F_b$ ) are applied at the base of the RC buildings where a connecting beam is considered. The uplift forces are applicable only in the cases where the inundation depth exceeds the height of the first floor (i.e. for the 4-storey and 9-storey MRFs). The amplitude of the tsunami forces increases with increasing inundation depth.

Different combinations of tsunami forces were considered according to FEMA (2008) prescriptions. More specifically, two different conditions were considered based on the hypothesis that the tsunami flow may or may not enter the building. In the first one tsunami flow cannot enter the building and cannot completely destroy the existing masonry infills, while in the second one it is assumed that tsunami flow can enter the building considering models without masonry infills. All tsunami loads were applied in proportion to each other assuming linearly increasing time-variant loads with a constant time step up to the (maximum) calculated values. The analyses are performed for different levels of inundation depth (at least 20 levels), varying from very small values (e.g.  $d=0.5\text{m}$ ), which result to negligible structural damage to large ones (e.g.  $d=10\text{m}$ ) which may lead to significant structural damages and potential collapse. Indicatively, numerical simulation of tsunami loading for the MRF 4-storey bare-frame and the infilled RC building is presented in Fig.3.

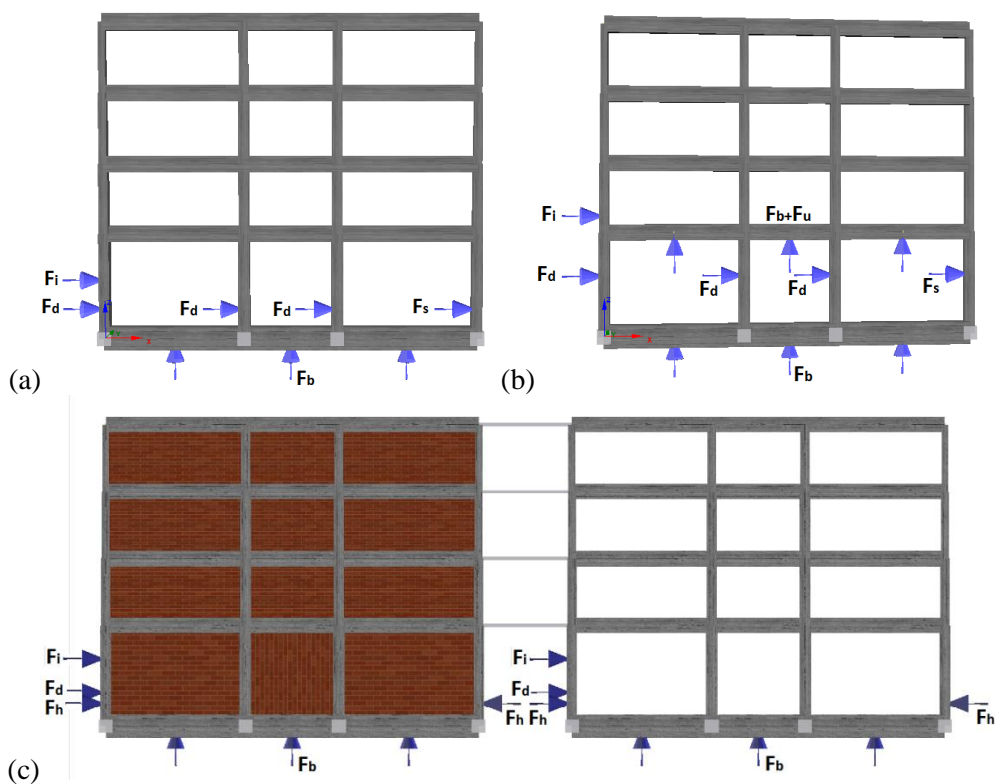


**Figure 3.** Numerical simulation of tsunami loading for the MRF 4-storey (a) bare-frame where  $d$  is lower than the height of the first floor, (b) bare-frame where  $d$  is higher than the height of the first floor (uplift forces are applicable) and the (c) infilled RC building

## FRAGILITY CURVES

### Definition of limit damage states

The definition of realistic limit damage states is of paramount importance for the construction of fragility curves. The selection of appropriate EDP to correlate with the selected IM (inundation depth) is a real challenge, as a suitable EDP has not yet been established in literature. When a building response to tsunami comprises structural damage, damage states can be classified using the same schemes used for structural damage triggered by an earthquake. However, the use of a global damage index such as the interstorey drift is not appropriate to be used as a tsunami EDP as the expected deformed shape and damage mechanism of the structure impacted by a tsunami is quite different from that of the same structure subjected to ground shaking. Thus, a local damage index in terms of building's material strain can be used as it shows an improved correlation with structural damage (Macabuag et al., 2014). Four limit states (LS1, LS2, LS3 and LS4) are defined based on nonlinear static analyses (tsunami time history analyses) for the various structure typologies, engineering judgment and the available literature (e.g. NIBS, 2004; Crowley et al., 2004; Fotopoulou and Pitilakis 2013). They describe the exceedance of minor, moderate, extensive and complete damage of the structures. According to (NIBS, 2004), "Steel Light Frames" structures are mostly single storey structures combining rod-braced frames in one direction and moment frames in the other. Due to the repetitive nature of the structural systems, the type of damage to structural members is expected to be rather uniform throughout the structure. Consequently, warehouses are considered as "Steel Light Frames" structures. A qualitative description of each damage state for reinforced concrete frames and warehouses is provided in Crowley et al. (2004) and NIBS (2004) for the RC buildings and the steel light frames respectively. The limit state values finally adopted are presented in Table 1.

**Table 1.** Definition of limit states for the different structure typologies considered

Limit states	Steel strain ( $\epsilon_s$ )			
	MRF bare frames	MRF with infills	Dual with/without infills	Warehouse
<i>Limit state 1</i>	0.002	0.0007	0.002	0.00112
<i>Limit state 2</i>	0.0125	0.002	0.0125	0.0125
<i>Limit state 3</i>	0.025	0.010	0.04	0.03
<i>Limit state 4</i>	0.045	0.020	0.08	0.055

In order to minimize the uncertainties associated with the selection of the appropriate damage state limits, nonlinear static analyses are performed for the different structures to define structure-specific limit state values (in terms of strains) for each damage state. Indicatively, Fig.4 illustrates the definition of limit states on the corresponding tsunami capacity curves derived from the tsunami nonlinear static analyses for some representative structure typologies. It is noted that the tsunami capacity curves are not extracted from a single nonlinear static analysis as for a seismic capacity curve (derived from a pushover analysis) but from the total number of the tsunami nonlinear static time history analyses. This is done considering that the location and amplitude of the applied tsunami forces changes as a function of the inundation depth. It is seen that for all analysis cases, steel strain ( $\epsilon_s$ ) gives more critical results. Hence, hereafter, the proposed limit damage states are defined in terms of steel bar strain. In particular, for the MRF models with bare frames the first limit state is specified as steel bar yielding while for the infilled ones the infills cracking is assigned as the first limit state and steel bar yielding as the second one. For the rest limit states, mean values of post-yield limit strains for steel reinforcement are suggested. For the dual models, the steel strain limits considered in MRF models cannot be used to characterize the extensive and complete damage of the dual systems, as they lead to lower levels of top displacement on the capacity curve. Thus, increased values of steel bar strain limits were adopted. It should be noted that the behaviour of the dual models when considering or not infills does not change considerably. This is to be expected considering that the contribution of the infills to the total stiffness of the model is small compared to that of the shear-wall. Based on the above considerations, the same limit strain values were specified for both bare and infilled dual structures. The same procedure is followed for the definition of the limit state values for the warehouse (steel light frame structures).

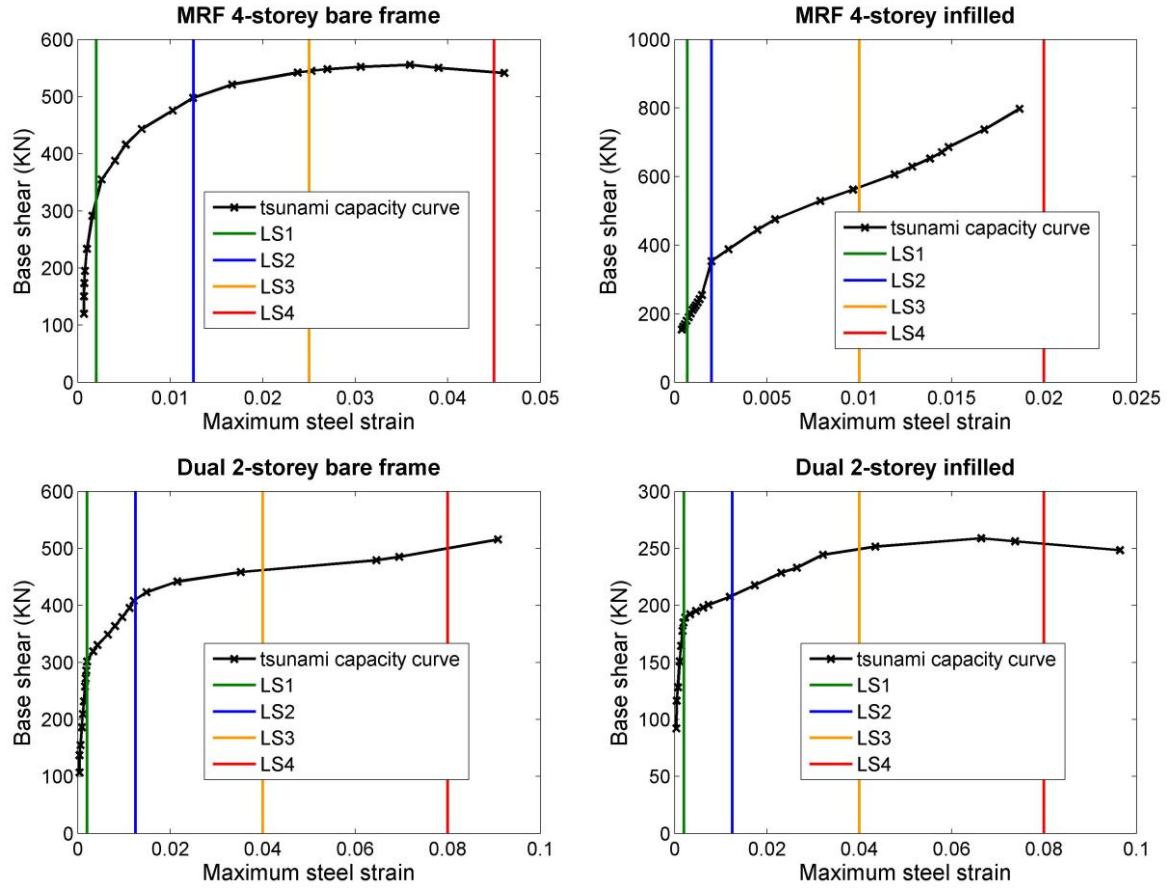


**Figure 4.** Definition of limit states on tsunami capacity curves for different structure typologies

### Construction of fragility curves

Fragility curves describe the probability of exceeding predefined levels of damage under a tsunami event of a given intensity. The results of the nonlinear numerical analysis (inundation depth - steel strain values) are used to derive fragility curves expressed as two-parameter lognormal distribution functions. Equation 1 gives the cumulative probability of exceeding a DS conditioned on a measure of the tsunami intensity IM:

$$P[DS_i/IM]=\Phi\left(\frac{\ln(IM)-\ln(IM_i)}{\beta}\right) \quad (1)$$

where,  $\Phi$  is the standard normal cumulative distribution function, IM is the intensity measure of the tsunami expressed in terms of inundation depth and  $\beta$  are the median values (in units of m) and log-standard deviations respectively of the building fragilities for each damage state  $i$  and  $DS_i$  is the damage state. The median values of inundation depth corresponding to the prescribed damage states are determined based on a regression analysis of the nonlinear static analysis results (inundation depth - steel strain pairs) for each structural model. More specifically, a second order polynomial fit of the logarithms of the inundation depth - steel strain data, which minimizes the regression residuals, is adopted in all cases.

The various uncertainties are taken into account through the log-standard deviation parameter  $\beta$ , which describes the total dispersion related to each fragility curve. The primary sources of uncertainty, which contribute to the total variability for any given damage state are those associated with the capacity of each structural type and the demand. The log-standard deviation value in the definition of the capacity is assumed to be equal to 0.3 for low code buildings (NIBS, 2004). The uncertainty in the demand is considered by calculating the dispersion of the logarithms of inundation depth - steel strain simulated data with respect to the regression fit (Cornell et al., 2002; Fotopoulou & Pitilakis, 2013). Under the assumption that these two log-standard deviation components are statistically independent, the total log-standard deviation is estimated as the root of the sum of the squares of the component dispersions. The computed log-standard deviation  $\beta$  values

of the curves vary from 0.33 to 0.57 for all structural models. Fig.5a and 5b illustrate the computed sets of fragility curves for the RC building typologies and the warehouse respectively with their lognormal distributed fragility parameters (median  $m$  and log-standard deviation  $\beta$ ) in terms of inundation depth.

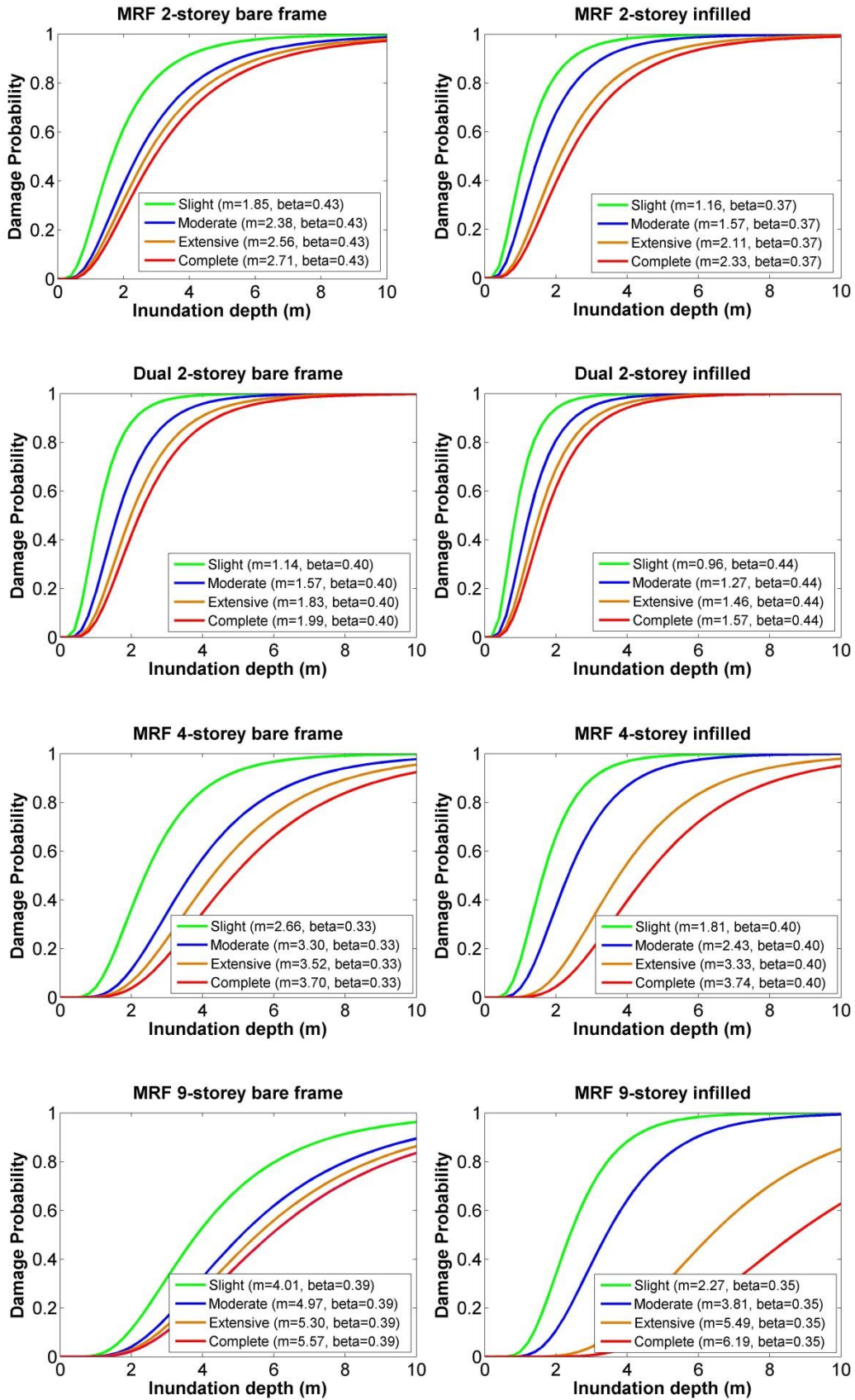


**Figure 5a.** Fragility curves for the different structure typologies considered



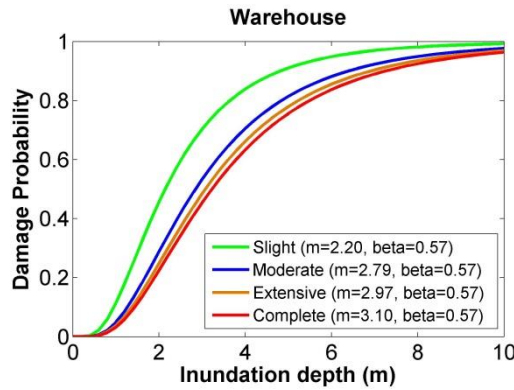


**Figure 5b.** Fragility curves for the warehouse

The numerical tsunami fragility curves have been compared with the few available empirical ones (Suppasri et al., 2013) obtained using field survey data from the 2011 Great East Japan tsunami for RC structures. Unfortunately the typology of RC buildings in Japan and Greece is not that same and the definition of damage states is also different. However if we will make the comparison for the complete damage state, where the definition of damage states is comparable, the comparison between the numerical and empirical curves is rather good (Fig.6). In particular, the proposed fragility curves for complete damage state stands between the empirical ones for complete and collapse damage states. The differences can be attributed to different parameters both methodological and the fact that the empirical fragility curves chosen for comparison were constructed based on hazard-damage relationships from previous tsunami events and expert judgment and they are highly specific to a particular seismo-tectonic, geotechnical and built environment. In addition, the proposed fragility curves refer to low code RC buildings in contrast to the empirical ones that include RC buildings of different design codes. Moreover, the empirical curves have been derived based on damage data from various RC building typologies while in our case representative MRF and dual typologies have been studied. Thus the empirical curves are characterised by a higher level of uncertainty indicated by the higher slope of the curves. Therefore, only preliminary comparisons can be made.

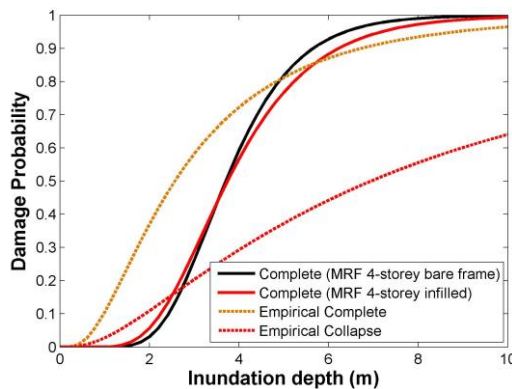


**Figure 6.** Comparison of the numerical tsunami fragility curves for the MRF 4-storey bare-frame and the infilled building with the empirical ones of Suppasri et al., (2013) for RC-structures

## CONCLUSIONS

Analytical tsunami fragility functions have been developed for various types of low-code RC buildings and a typical warehouse. An extensive numerical parametric investigation has been performed considering different combinations of statically applied tsunami loads for gradually increasing tsunami inundation depths for various typologies representative of typical Thessaloniki's port structures. Structural limit states have been defined in terms of threshold values of material strain based on nonlinear static analyses results. Fragility curves have been derived for different inundation depths and for the various structure typologies.

It has been shown that the high-rise RC buildings have lower vulnerability compared to the low-rise ones. The low-rise and mid-rise models with infills are more vulnerable compared to the bare frames. This trend also holds true for the high-rise MRF for the exceedance of slight and moderate damage. This is in accordance with

the FEMA guideline, which recommends the design of vertical evacuation buildings with break-away walls or open construction in the lower levels to allow water to pass through with minimal resistance. In contrast, when extensive or complete damage of the structures is anticipated, the bare frame is expected to sustain larger damages compared to the infilled one. This could be due to the fact that, for the high-rise building, the infills of the upper floors are less affected by the tsunami waves making the remaining resistance of the infilled building higher compared to the bare frame for extensive and complete damage states. Moreover, the low-rise dual models are more vulnerable compared to the MRFs, which is related to the concentration of large tsunami forces to shear walls. This is the reason why FEMA recommends for the design of vertical evacuation structures, shear walls be oriented parallel to the anticipated direction of tsunami flow to reduce associated tsunami forces. Regarding the fragility curves for the warehouse they are generally similar to the ones of the low-rise and mid-rise MRF RC buildings. It is also observed that the difference between the damage states is not so large indicating that once yielding occurs, the structure very rapidly attains the post-yield limit states. A preliminary comparison between the numerical tsunami fragility curves and the few available empirical ones (Suppasri et al., 2013) obtained using field survey data from the 2011 Great East Japan tsunami for RC-structures has been made enhancing the reliability of the proposed curves. The proposed fragility curves could be used within a probabilistic risk assessment framework to assess the vulnerability of low-code RC buildings and typical steel warehouses exposed to tsunami hazard. Knowing the expected tsunami height from an appropriate tsunami hazard analysis and the structural characteristics of the exposed structures one could make use of the appropriate set of fragility curves to assess the expected damage state and finally take adequate decisions to reduce, if necessary, the risk.

## REFERENCES

- Cornell CA., Jalayer F., Hamburger RO., Douglas AF. Probabilistic basis for 2000 SAC federal emergency management agency steel moment frame guidelines. *Journal of Structural Engineering*, 2002, 128(4): 526-533.
- Crisafulli F. Seismic Behaviour of Reinforced Concrete Structures with Masonry Infills. (PhD Thesis ed.). 1997, University of Canterbury, New Zealand.
- Crowley H., Pinho R., & Bommer J. A probabilistic displacement-based vulnerability assessment procedure for earthquake loss estimation. *Bull Earthq Eng.*, 2004, 2:173–219.
- FEMA. Guidelines for Design of Structures for Vertical Evacuation from Tsunamis - Report P-646. 2008; Redwood City, CA: Federal Emergency Management Agency.
- Fotopoulou S. & Ptilakis K. Fragility curves for reinforced concrete buildings to seismically triggered slow-moving slides. *Soil Dynamics and Earthquake Engineering*, 2013, 48:143–161.
- Kappos A., Panagopoulos G., Panagiotopoulos C., & Penelis G. A hybrid method for the vulnerability assessment of R/C and URM buildings. *Bull Earthq Eng.*, 2006, 4:391–419.
- Koshimura S., Oie T., Yanagisawa H., & Imamura F. Developing fragility functions for tsunami damage estimation using numerical model and post-tsunami data from Banda Aceh, Indonesia”, *Coastal Engineering Journal*, 2009, 51:243–273.
- Macabuag J., Lloyd T., & Rossetto T. Towards the development of a method for generating tsunami fragility functions. *Proceedings of 2<sup>nd</sup> European Conference on Earthquake Engineering and Seismology 2014*; Istanbul.
- Mander J. Theoretical stress-strain model for confined concrete. *J Struct Eng.*, 1988, 114:1804–1826.
- Mas E., Koshimura, S., Suppasri A., Matsuoka M., Matsuyama M., Yoshii T., Jimenez C., Yamazaki F., & Imamura F. Developing Tsunami fragility curves using remote sensing and survey data of the 2010 Chilean Tsunami in Dichato. *Nat. Hazards Earth Syst. Sci.*, 2012, 12:2689-2697.
- Neuenhofer A., & Filippou F. Evaluation of nonlinear frame finite-element models. *Journal of Structural Engineering*, 1997, 123:958-966.
- National Institute of Building Sciences (NIBS), 2004. Direct physical damage—general building stock. HAZUS-MH Technical manual, Chapter 5. Federal Emergency Management Agency, Washington, D.C
- Ptilakis K. Vulnerability Assessment of RC Buildings. Present State and Challenges, Keynote Lecture at 8<sup>th</sup> Turkish National Conference in Earthquake Engineering, 11-15 May 2015, Istanbul, Turkey.
- Reese S., Bradley BA., Bind J., Smart G., Power W. & Sturman, J. Empirical building fragilities from observed damage in the 2009 South Pacific tsunami, *Earth-Science*, 2011, Reviews. 107:156–173.
- SeismoSoft. A computer program for static and dynamic nonlinear analysis of framed structures. (SeismoStruct, Ed.) 2015, Retrieved from www.seismosoft.com
- Suppasri A., Koshimura S. & Imamura F. Developing tsunami fragility curves based on the satellite remote sensing and the numerical modeling of the 2004 Indian Ocean tsunami in Thailand. *Natural Hazards Earth System Science*, 2011, 11:173-189.
- Suppasri A., Mas E., Charvet I. & Gunasekera R. Building damage characteristics based on surveyed data and fragility curves of the 2011 Great East Japan tsunami. *Nat Hazards*, 2013, 66:319–341.